Solar Energy
And Sustainable Development
Refereed, biannual scientific journal issued by:
The Libyan Center for Solar Energy Research and Studies

Numerical Investigation on Mixed Convection Phenomenon Within a 2D Cavity Shaped Home Containing Solar Chimney

Mahmoud Kalfali[1*], Mouna Maache Battira[2], Nourredine Belghar[3], Chihab Eddine Brahmi[4].

[1,2,3,4]Department of Mechanical Engineering, ABBES LAGHROUR University Khenchela, Algeria.
[1]Laboratory of Studies of Industrial Energy Systems LESEI, Faculty of Technology, University of Batna 2, Batna, Algeria.

E-*mail:* [1] kalfali.mahmoud@univ-khenchela.dz ,[2] mouna.maache@univ-khenchela.dz ,[3] N.belghar@univ-biskra.dz , [4] ybrahmi.chihabeddine@univ-khenchela.dz .

ARTICLE INFO.

Article history:
Received 20 Feb 2025
Received in revised form 25 Feb 2025
Accepted 15 May 2025
Available online 22 May 2025

KEYWORDS

Mixed convection, Solar chimney, Home, Cavity, Ventilation.

ABSTRACT

This study investigates the numerical simulation of mixed convection within a two-dimensional cavity shaped like a solar chimney in a home configuration. The primary goal is to investigate airflow and heat transfer effects to optimize solar chimney performance for residential applications. The analysis incorporates various parameters, such as Richardson (Ri) and Reynolds (Re) numbers, along with two distinct ventilation inlet positions: Case 1 at (x=0, y=0.9) and Case 2 at (x=0, y=0.1).

Simulations are performed using a numerical code based on the Galerkin finite element method and the Boussinesq approximation. The findings suggest that an upper ventilation location significantly enhances airflow circulation and improves heat transfer by 20% compared to lower ventilation. For Ri values within 2.5≤Ri<5, forced convection is predominant, accelerating airflow velocity by 35%. In contrast, at Ri=10, natural convection takes over, creating a 40% higher thermal gradient. Additionally, an increase in Reynolds number from 100 to 500 results in a 25% improvement in convective heat transfer. Lastly, the solar chimney configuration boosts ventilation efficiency by 30%, underscoring its potential to enhance indoor air quality in residential buildings.

*Corresponding author.

DOI: https://doi.org/10.51646/jsesd.v14i1.467

دراسة عددية لظاهرة الحمل الحراري المختلط داخل منزل على شكل تجويف ثنائي الأبعاد يحتوي على مدخنة شمسية

محمود كلفالي، منى معاش بطيرة, نور الدين بلغار, شهاب الدين براهمي.

ملخص: تبحث هذه الدراسة في المحاكاة العددية للحمل الحراري المختلط داخل تجويف ثنائي الأبعاد على شكل مدخنة شمسية في تصميم منزل. الهدف الرئيسي هو دراسة تأثيرات تدفق الهواء ونقل الحرارة لتحسين أداء المدخنة الشمسية للتطبيقات السكنية. يتضمن التحليل معلمات مختلفة، مثل أرقام ريتشاردسون ورينولدز، إلى جانب وضعين متميزين لمدخل التهوية: الأول عند (x=0, y=0.9)، والثاني عند. (x=0, y=0.1) يتم إجراء المحاكاة باستخدام رمز عددي يعتمد على طريقة العناصر المحدودة لغالركين وتقريب بوسينسك. تشير النتائج إلى أن موقع التهوية العلوي يعزز بشكل كبير دوران تدفق الهواء ويحسن نقل الحرارة بنسبة 20٪ مقارنة بالتهوية السفلية. بالنسبة لقيم Ri ضمن 2.5≤Ri<5، يكون الحمل الحراري القسري هو السائد، مما يؤدي إلى تسريع سرعة تدفق الهواء بنسبة 35%. في المقابل، عند قيمة Ri=10، يسود الحمل الحراري الطبيعي، مما يزيد التدرج الحراري بنسبة 40 %. إضافةً إلى ذلك، تؤدي زيادة رقم رينولدز من 100 إلى 500 إلى تحسن بنسبة 25% في انتقال الحرارة بالحمل الحراري. وأخيرًا، يعزز تصميم المدخنة الشمسية كفاءة التهوية بنسبة 30% ، مما يؤكد قدرتها على تحسين جودة الهواء الداخلي في المباني السكنية.

الكلمات المفتاحية – الحمل الحراري المختلط، المدخنة الشمسية، منزل، التجويف، التهوية.

1. INTRODUCTION

In 2023, residential energy consumption accounted for approximately 30% of total energy consumption in the world and contributed approximately 27% of total greenhouse gas emissions. The situation is very different in developing countries, where residential sector consumption may up to 60%. [1] In Algeria, the residential sector is estimated to consume approximately 39% of the country's electricity and contributed approximately 18.7% of total greenhouse gas emissions. It is therefore responsible for an estimated 28.2 Mtons of CO2 annually. [2] In light of the growing challenges associated with rising energy consumption and the depletion of traditional resources, there is an increasing need to adopt sustainable and efficient solutions in the residential sector, which is one of the largest energy-consuming sectors. Solar energy technologies, whether passive systems based on architectural design such as natural ventilation and solar lighting, or active systems like photovoltaic panels and solar water heaters, are among the most promising solutions to achieve this goal. Integrating these technologies helps reduce dependence on fossil fuel sources, lowers long-term economic costs, and mitigates harmful emissions that negatively impact the environment. Therefore, adopting solar energy systems in residential buildings is not only an environmental choice but also an economic and strategic necessity on the path to achieving sustainable development. [3]

The integration of solar energy into building design has become a key focus in sustainable architecture, attracting growing interest in recent years. "Solar architecture" refers to an approach that seamlessly incorporates solar technologies into buildings to optimize energy utilization. [4] This concept merges architectural design with advanced solar systems to enhance energy efficiency and sustainability. There are multiple strategies for integrating solar energy into buildings. One method involves the implementation of building-integrated solar thermal systems (BISTs) and building-integrated photovoltaic systems (BIPVs). [5] BISTs contribute to heating, cooling, and domestic hot water supply, whereas BIPVs facilitate electricity generation [6]. Another innovative approach incorporates a modular, multi-layered combination of building shielding, insulation, and solar energy collection components. [7] This study is particularly significant in regions with hot climates, as it helps reduce dependence on artificial air conditioning, leading to lower energy consumption and reduced carbon emissions. By adopting solar energy solutions, this study

aims to promote sustainable building practices and achieve more efficient energy consumption, supporting efforts toward a more sustainable and eco-friendly environment. [8] Compared to conventional photovoltaic/thermal (PV/T) systems, this design improves thermal efficiency by approximately 8.49% and electrical efficiency by 0.31%. [9]

Solar chimneys operate through three key components: transparent glazing, an air cavity, and a solar-absorbing wall. When sunlight penetrates the glazing, it heats the air within the cavity by transferring energy from the absorbing wall Nguyen et al. [10] Additionally, integrating thermal energy storage and passive heating techniques can further optimize the performance of solar chimneys, offering an energy-efficient alternative to conventional climate control systems Ibrahim et al. [11] This thermal buoyancy effect efficiently expels hot air while drawing in fresh air, significantly improving airflow within the building. By incorporating techniques such as thermal energy storage and passive heating, solar chimneys enhance both cooling and heating efficiency. Salamah et al. [12] carried out a techno-economic study on solar energy technologies in Libyan residential areas, concentrating on solar water heating systems and grid-connected photovoltaic setups. This research is significant due to its practical and data-driven analysis of the feasibility of renewable energy solutions in Libya, especially in light of the country's ongoing energy challenges. The results showed considerable long-term cost savings and a significant reduction in CO_2 emissions, emphasizing the importance of solar technologies in aiding the transition to sustainable, low-carbon energy systems. Consequently, this study provides a valuable resource for research focused on enhancing energy efficiency and promoting the integration of renewable energy in regions with abundant sunlight.

Their effectiveness is particularly notable in regions with extreme climates, where they help reduce energy consumption while maintaining indoor comfort. [13,14] This study examines the performance and potential of solar chimneys for both cooling and ventilation, especially when integrated with additional energy-efficient strategies. Their benefits are particularly significant in regions with harsh climates, where they contribute to reduced energy consumption while maintaining indoor thermal comfort Brito-Coimbra et al. [15] Furthermore, the investigation of solar chimney power plants (SCPP) relies on a thorough understanding of heat transfer phenomena. Several studies have analyzed the underlying heat transfer mechanisms. For instance, a numerical study conducted by Brahmi et al. [16] examined natural convection within square porous irregular cavities using the Galerkin finite element method. The findings revealed that sinusoidal vertical walls enhance heat transfer more effectively compared to concave or convex walls. Additionally, another numerical analysis by Brahmi et al. [17] explored the geothermal performance of optimal soil properties for greenhouse applications. This study modeled steady free convection within a two-dimensional cavity, partially filled with a porous layer, incorporating three embedded hot pipes beneath a semi-elliptical upper boundary. Using the Galerkin finite element method, the research analyzed parameters such as Rayleigh numbers, Darcy numbers, and porosity. The results indicated that heat transfer improves with increasing Rayleigh numbers and permeability, while Darcy numbers significantly influence heat transfer at higher Rayleigh values.

To explore the impact of solar chimneys and mixed convection on improving natural ventilation and energy efficiency in buildings, a mathematical model was developed to evaluate the performance of a solar chimney, taking into account both thermal and geometric considerations. Their experiments tested a prototype under different conditions, examining air velocity and temperature variations based on solar radiation. Bassiouny et al. [18] investigated the impact of chimney inlet size and width on ventilation. Their numerical analysis revealed that chimney width has a greater effect on the air change rate (ACH) than inlet size. Kalfali et al. [19] studied solar chimney ventilation under mixed convection, highlighting its potential for sustainable building

design. Shi et al. [20] Conducted a comprehensive study to identify the key factors influencing the performance of solar chimneys in buildings. Their research examined various design parameters, environmental conditions, and operational aspects affecting ventilation efficiency and thermal performance. The study highlighted critical factors such as chimney height, width, absorber material, glazing type, and ambient temperature. The findings indicate that optimizing these parameters can significantly enhance airflow rates and energy efficiency. Additionally, the study emphasized the importance of integrating solar chimneys with other passive ventilation strategies to improve building sustainability.

Ali J. Chamkha et al. [21] examined mixed convection in a vented cavity, demonstrating that increased airflow enhances heat transfer, thereby improving ventilation performance. Understanding mixed convection is crucial for optimizing natural ventilation, reducing energy consumption, and enhancing indoor air quality. Our study will focus on solar chimneys and propose integrating turbines to generate electricity, contributing to more energy-efficient and sustainable buildings. Saha et al. [22] investigated mixed convection in an enclosure with different inlet and exit configurations. Their study analyzed how airflow patterns and heat transfer are influenced by various inlet and outlet placements. The results showed that the configuration of these openings significantly affects temperature distribution and convection efficiency. The research provides insights into optimizing ventilation and cooling performance in enclosed spaces. Rahman et al. [23] conducted a numerical study on mixed convection in a square cavity containing a heat-conducting square cylinder placed at different locations. Their research examined how the position of the cylinder affects heat transfer and fluid flow within the cavity. The findings revealed that cylinder placement plays a crucial role in convection efficiency, influencing temperature distribution and circulation patterns. This study contributes to the optimization of thermal management in enclosed spaces.

Through this research, our study will highlight the crucial role of mixed convection in home ventilation, focusing on the use of solar chimneys to enhance and strengthen air movement within inhabited spaces. We will examine how mixed convection promotes the efficiency of natural ventilation by optimizing airflow through the chimneys. Additionally, we propose the integration of turbines into these solar chimney systems, allowing for the generation of electrical energy for homes. This approach not only harnesses the movement of air within the chimney but also contributes to a more sustainable use of energy resources while improving indoor air quality and thermal comfort for occupants. By combining these elements, our study aims to demonstrate how mixed convection and innovative ventilation technologies can play a key role in the design of more sustainable and energy-efficient homes.

2. COMPUTATIONAL MODEL DESCRIPTION

2.1. Physical model configuration

Figure 1 depicts the configuration under study, which features a cavity designed to simulate a house equipped with a solar chimney. In this arrangement, the hot wall of the house is situated next to the thermal chimney, while the cold wall at the inlet is exposed to incoming airflow at a predetermined temperature. The primary objective of this study is to investigate the effect of the inlet location on the efficiency of ventilation within the house. By analyzing how various inlet positions affect airflow dynamics, we aim to deepen our understanding of the natural ventilation mechanisms inherent in this architectural design.

The dimensions of the house are specified as follows: the length (L = 1) is equal to the height of the solar chimney, and the inlet width is (W=d = 0.1L), which also corresponds to the gap between the chimney and the house. Additionally, the house is topped with a dome that has a

height of (h = 0.2L).

To streamline the physical model while maintaining accuracy, the flow is assumed to be two-dimensional, steady-state, and laminar. The fluid is considered incompressible, with thermophysical properties remaining constant, except for density, which is assumed to vary linearly with temperature according to the Boussinesq approximation. This approximation is applied within the fluid domain and in the volumetric force terms. The analysis incorporates a Prandtl number of (Pr = 0.71), a Reynolds number ranging from 100 to 500, and a Richardson number varying between 2.5, 5 and 10. These parameters facilitate an efficient assessment of the governing thermal and flow dynamics.

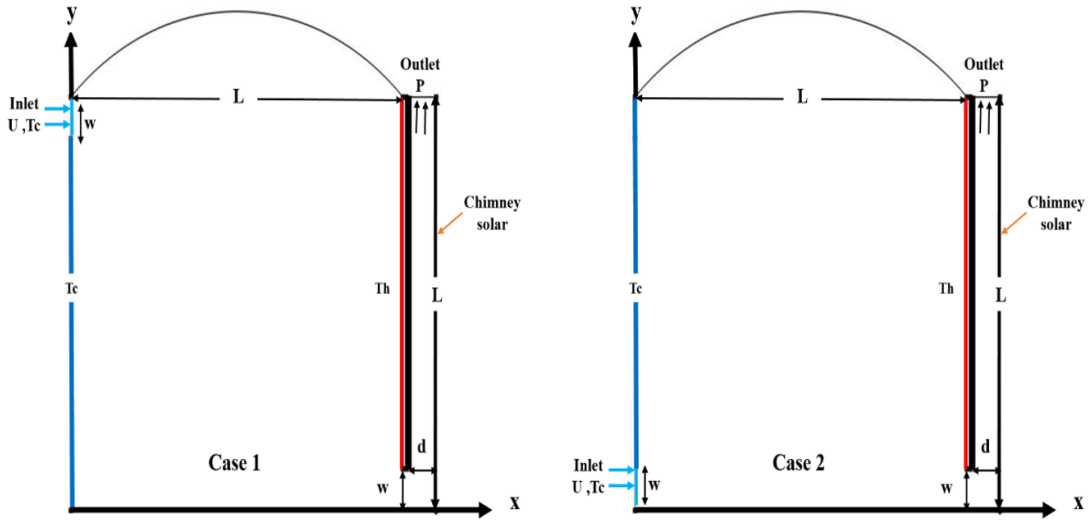

Figure 1. Schematization of the physical model.

2.2. Mathematical formulation

Based on the assumptions outlined above, the governing equations for the flow are the continuity, momentum, and energy equations. These equations can be expressed in their dimensional form as follows [23]:

Continuity equation:

$$\frac{\partial u}{\partial x}+\frac{\partial v}{\partial y}=0 \qquad (1)$$

Momentum equations along x and y axis:

$$u\frac{\partial u}{\partial x}+v\frac{\partial u}{\partial y}=-\frac{1}{\rho}\frac{\partial P}{\partial x}+\frac{\mu}{\rho}\left(\frac{\partial^2 u}{\partial x^2}+\frac{\partial^2 u}{\partial y^2}\right) \qquad (2a)$$

$$u\frac{\partial v}{\partial x}+v\frac{\partial v}{\partial y}=-\frac{1}{\rho}\frac{\partial P}{\partial y}+\frac{\mu}{\rho}\left(\frac{\partial^2 v}{\partial x^2}+\frac{\partial^2 v}{\partial y^2}\right)+\beta g(T-Tc) \qquad (2b)$$

Energy equation:

$$u\frac{\partial T}{\partial x}+v\frac{\partial T}{\partial y}=\alpha\left(\frac{\partial^2 T}{\partial x^2}+\frac{\partial^2 T}{\partial y^2}\right) \qquad (3)$$

The formulations for the reduced variables used in the dimensioning of equations (1-3), as well as the Reynolds, Grashof, Prandtl, and Richardson numbers, are as follows [24]:

$$X=\frac{x}{L};\ Y=\frac{y}{L};\ \theta=\frac{T-Tc}{Th-Tc};\ U=\frac{u}{U_o};\ V=\frac{v}{U_o};$$

$$Re=\frac{U.H}{\vartheta};\ Gr=\frac{g.\beta(Th-Tc)H^3}{\vartheta^2},\ Pr=\frac{Gr}{Re^2}$$

The dimensionless governing equations are expressed as follows [24,25]:

$$\frac{\partial U}{\partial X}+\frac{\partial V}{\partial Y}=0 \qquad (4)$$

$$U\frac{\partial U}{\partial X}+V\frac{\partial U}{\partial Y}=-\frac{\partial P}{\partial X}+\frac{1}{Re}\left(\frac{\partial^2 U}{\partial X^2}+\frac{\partial^2 U}{\partial Y^2}\right) \qquad (5)$$

$$U\frac{\partial V}{\partial X}+V\frac{\partial V}{\partial Y}=-\frac{\partial P}{\partial Y}+\frac{1}{Re}\left(\frac{\partial^2 V}{\partial X^2}+\frac{\partial^2 V}{\partial Y^2}\right)+Ri.\theta \qquad (6)$$

$$U\frac{\partial \theta}{\partial X}+V\frac{\partial \theta}{\partial Y}=\frac{1}{Re.Pr}\left(\frac{\partial^2 \theta}{\partial X^2}+\frac{\partial^2 \theta}{\partial Y^2}\right) \qquad (7)$$

The expression for the avarge Nusselt number is given by [26]:

$$Nu=-\frac{\partial \theta}{\partial n} \qquad (8)$$

Where, $\frac{\partial}{\partial n}$ denotes the non-dimensional derivative in the direction perpendicular to the surface in consideration and the I below represents the length of the wall.
The expression for the avarge Nusselt number is given by [26]:

$$Nu_{avg}=-\frac{1}{l}\int_0^l Nu.dx \qquad (9)$$

2.3. Boundary Conditions

To achieve a realistic simulation of flow and heat transfer, appropriate boundary conditions are integrated into the computational model. The specific boundary conditions implemented in the model include the following:

The inlet boundary conditions are specified at two points: Case 1 at (x = 0, y = 0.9) and Case 2 at (x = 0, y = 0.1). For both cases, the velocity components are defined as U = 1 and V = 0, with the temperature θ set to 0.

At the outlet boundary located at (x = 1.1, y = 1), the pressure is specified as P=0.

The boundary conditions are defined as follows: at the cold wall located at (x = 0, y = 1), both velocity components (U and V) are zero, and the temperature, θ, is also zero. Meanwhile, at the hot wall positioned at (x = 1, y = 1), the velocity components remain U= V = 0, but the temperature increases to θ = 1.

Inlet:	U=1,V=0 and θ=0	(10a)
Cold wall:	U=V=0 and θ=0	(10b)
Hot wall:	U=V=0 and θ=1	(10c)
Outlet :	Pressure P=0	(10d)

3. NUMERICAL SIMILATION

We have used COMSOL Multiphysics®, a commercial software based on the finite element technic. The governing Equations (4-7), including the set of boundary conditions as mensioned in the section 2.3, were treated. Where the mesh inside the computational model follows a triangular grid, we use the weak form of the governing equations using the (GFEM) Galerkin finite element method. Velocity components and pressure are Discretized choosing P2–P1 Lagrange finite elements with Lagrange-quadratic finite elements for the temperature.

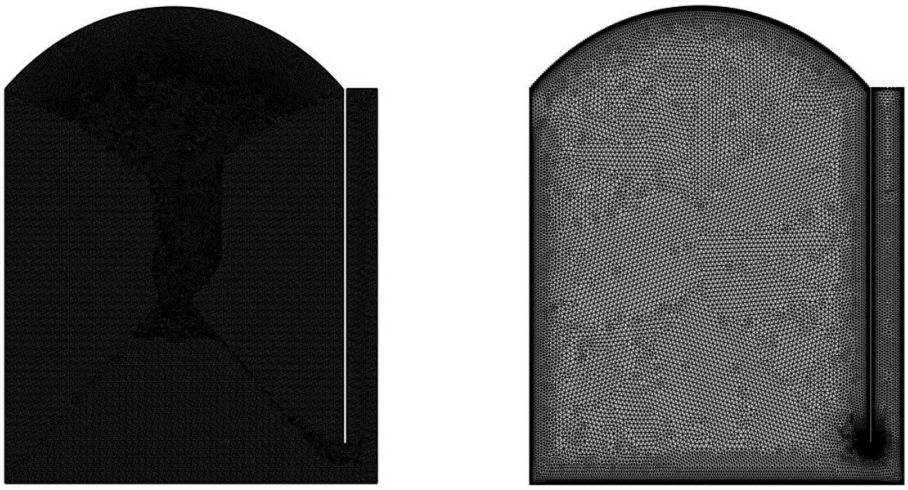

Figure 2. Mesh representation of the computational domain.

Table 1. Flow characteristics for different grids (Ri=10, Re=100 and Pr=0.71).

Mesh	6055	108350	273570	305750
$\mathbf{Nu_{avg}}$	5.965	5.673	5.643	5.642

To evaluate the thermal performance of a solar chimney system, the average Nusselt number was determined using a cavity model that simulates a simplified house with an integrated thermal chimney. In this setup, the hot wall is positioned adjacent to the chimney, while the cold wall at the inlet is exposed to ambient air flow at a constant temperature. The numerical simulation utilized appropriate approximations within the fluid domain and accounted for the effects of volumetric forces. For a representative analysis, key dimensionless parameters were set at Ri = 10, Re = 100, and Pr = 0.71, detailed in Table 1. A triangular mesh structure (see Figure 2) was used to accurately capture the flow and thermal gradients within the cavity. A mesh of 305,750 elements was chosen based on independence testing to ensure both reliable results and computational efficiency.

3.1. Model validation

To assess the performance of the mixed convection network, we replicated the study conducted by Chamkha et al [21]. which analyzed mixed convection heat transfer within a square vented cavity containing a heated horizontal square cylinder. In this investigation, the airflow within the cavity was assumed to be two-dimensional, steady, and incompressible, with constant physical properties, except for density, which was treated using the Boussinesq approximation. The comparison specifically examines a scenario where the Richardson number (Ri) ranges from 2.5 to 10, the Prandtl number (Pr) is set at 0.71, and the Reynolds number (Re) is fixed at 50. The data points for this comparison are presented in Figure 3. The results indicate excellent agreement, with the values converging closely and exhibiting an extremely small margin of error.

This comparison not only validates our findings but also ensures consistency with established results in the field of mixed convection heat transfer, reinforcing the reliability of our analysis.

Table 2. Comparisons of the average Nusselt number (Chamkha et al.) present results at 2.5 ≤ Ri ≤ 10, Re = 200 and Pr = 0.71.

Ri	2.5	5	10
Nu_{avg} Chamkha et al.	2.119	2.500	2.890
Nu_{avg} present results	2.132	2.522	2.903

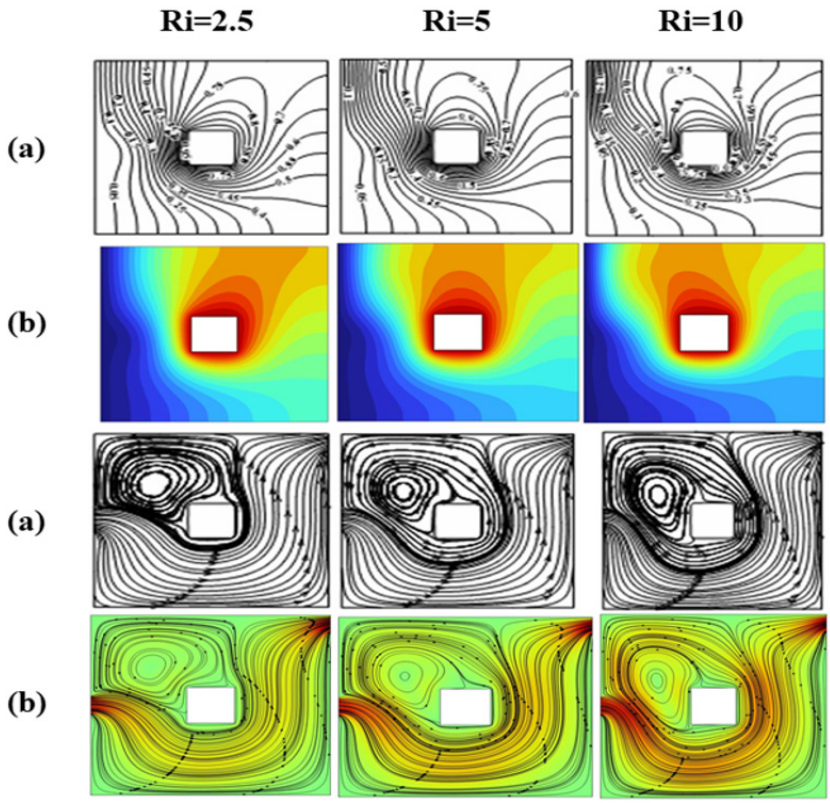

Figure 3. Comparisons of Stream function and temperature contours. (a) Chamkha et al [21]. (b) present results at 2.5 ≤ Ri ≤ 10, Re = 50 and Pr = 0.71.

4. RESULTS AND DISCUSSION

This section details the computational findings related to laminar convective flow and heat transfer in a home featuring a thermal chimney, analyzed across two distinct scenarios. The study explores the thermal interactions between natural and forced convection, with the hot wall adjacent to the thermal chimney and the cold air entering through the inlet influencing the flow dynamics. The results are presented through contours of velocity magnitude and isotherms, as well as isoclines of Stream function and the variation of the average Nusselt number. Additionally, the local Nusselt number is assessed over a range of Richardson numbers (2.5 ≤ Ri ≤ 10) and Reynolds number (Re) ranges from 100 to 500, offering valuable insights into the heat transfer characteristics of the system.

4.1. Discussion of velocity magnitude results

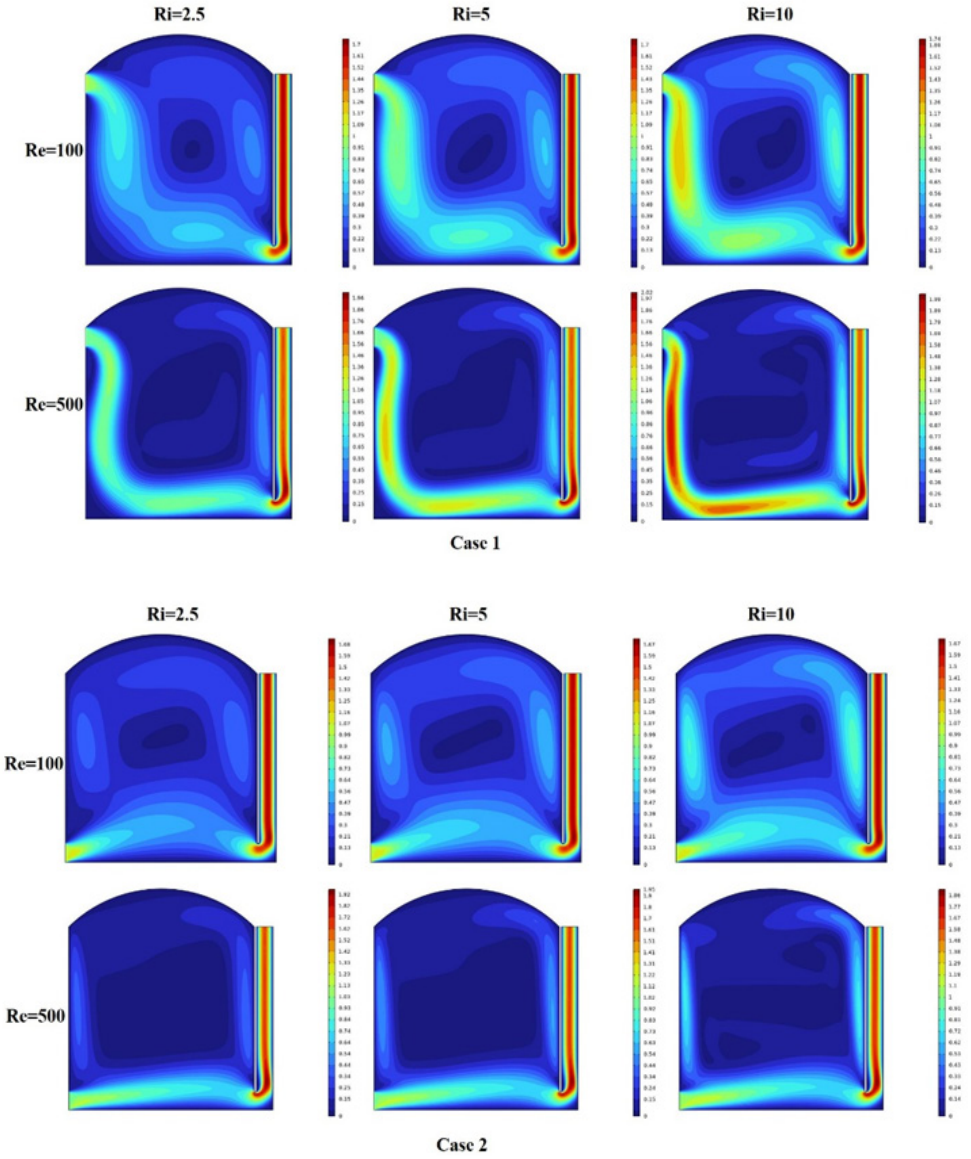

Figure 4. Velocity Magnitude for Both Cases at Pr = 0.71.

The results presented in Figure 4, which analyze both study cases concerning the position of the ventilation inlet, reveal significant variations in airflow dynamics. When the inlet is positioned at the top, the airflow inside the house follows a circular trajectory, with significantly higher velocities than in the second configuration, where the inlet is placed at the bottom. Moreover, the velocity within the thermal chimney reaches its maximum in the first case, which can be attributed to variations in pressure and temperature, as well as the chimney's function in enhancing ventilation and air circulation. Consequently, this configuration allows for a more effective evaluation of the air exchange rate within the indoor environment. Additionally, the findings underscore the impact of the Richardson number (Ri) on airflow behavior, particularly within the range of $2.5 \leq Ri \leq 10$. The results indicate that at lower Ri values within this range, forced convection is the dominant mechanism, leading to higher airflow velocities. As Ri increases, buoyancy forces gradually become more influential, causing a reduction in airflow velocity and shifting the flow characteristics toward natural convection dominance. Furthermore, the effect of the Reynolds number (Re) on airflow characteristics is evident. When comparing Re = 100

and Re = 500, a significant increase in air velocity is observed at the higher Reynolds number. This increase enhances air circulation and heat transfer efficiency, contributing to improved indoor ventilation. These results emphasize the critical role of both the Richardson and Reynolds numbers in governing airflow dynamics and highlight the intricate interaction between natural and forced convection in indoor ventilation systems.

4.2. Discussion of Stream function and temperature contours

In forced convection heat transfer, buoyancy effects are inherently present and interact with forced flow.

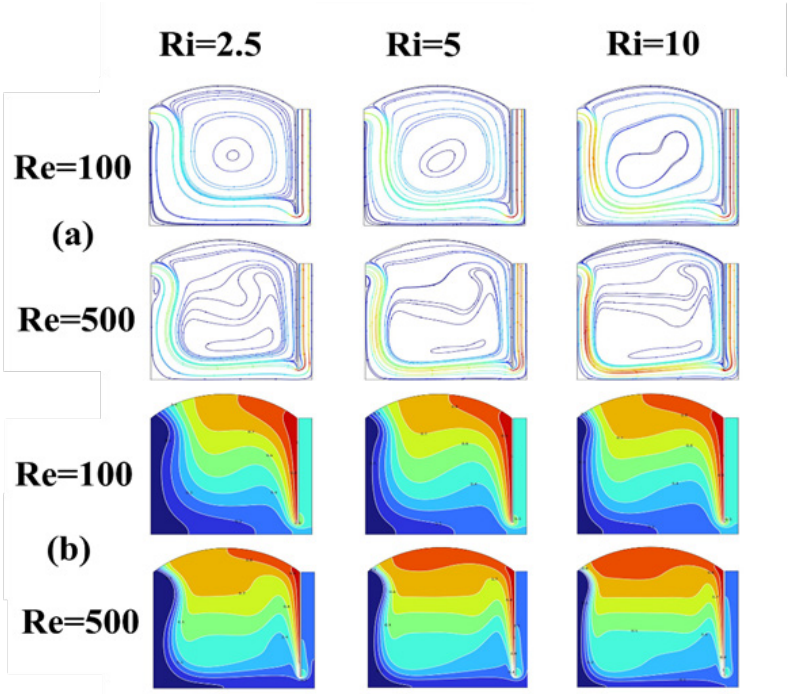

forced flow.

Figure 5. (a) Stream function, (b) temperature contours case 1 at Pr = 0.71.

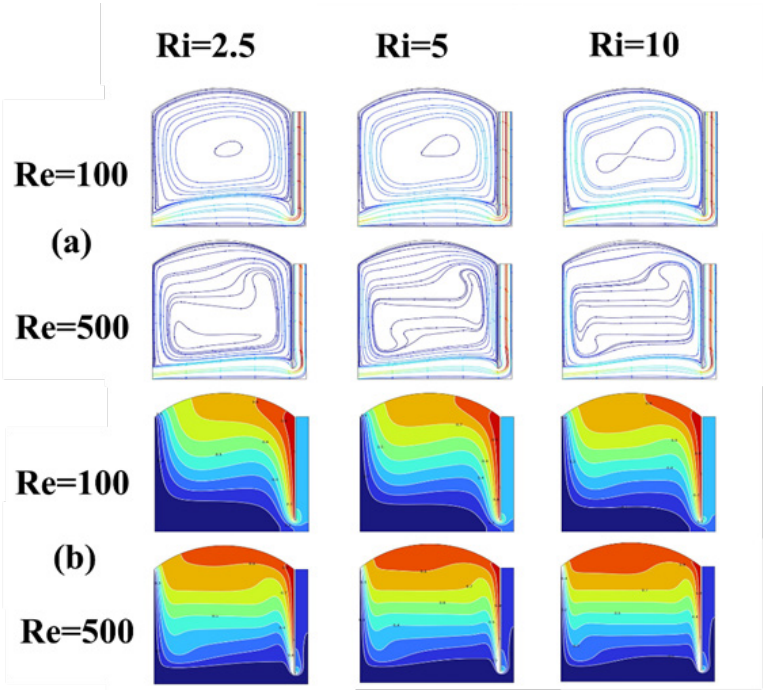

Figure 6. (a) Stream function, (b) temperature contours case 2 at Pr = 0.71.

When buoyancy forces are relatively weak, forced convection dominates the heat transfer process, whereas stronger buoyancy forces lead to the dominance of natural convection. In cases where both mechanisms contribute significantly to the flow behavior, the process is classified as mixed convection, with the Reynolds number (Re) and Richardson number (Ri) serving as the primary controlling parameters.

This study investigates the effect of Re and Ri on airflow dynamics inside a house-shaped cavity. The results presented in Figures (5.a) and Figures (6.a) illustrate the streamlines different values of Re and Ri under varying ventilation inlet conditions. The findings indicate that increasing Re mitigates the influence of the hot wall and enhances convective heat transfer. At Re = 100, a small vortex appears in the center of the cavity, which intensifies and expands with increasing Ri. When Re is increased to 500, the vortex structure evolves into a larger and more distinct pattern, highlighting the dominance of forced convection in shaping the airflow. Regarding Ri, at Ri = 2.5, buoyancy effects become more pronounced, promoting vortex formation within the cavity. As Ri increases to 5, the vortex size expands, particularly at Re = 500, due to enhanced buoyancy-driven effects. At Ri = 10, buoyancy forces predominantly govern the flow behavior, resulting in a convective regime primarily dictated by natural convection. These results emphasize the intricate interplay between forced and natural convection, underscoring the crucial roles of both Re and Ri in determining airflow patterns and heat transfer characteristics within the system. At the chimney, the velocity streamlines exhibit a linear and dense pattern, which becomes more pronounced as the Reynolds number (Re) increases. This behavior indicates that higher Re values enhance the flow momentum, leading to a more structured and intensified airflow within the chimney. The increased velocity facilitates the efficient removal of heated air, reinforcing the dominance of forced convection in this region. Consequently, as Re rises, the chimney plays a more significant role in expelling hot air, improving ventilation, and enhancing overall heat transfer efficiency within the system.

Figures (5.b) and Figures (6.b) show the distribution of isotherms for low Reynolds (Re) numbers (Re < 2000) and Richardson (Ri) under different ventilation inlet positions in the studied house model. The upper sections of these figures show a curved isotherm pattern, demonstrating heat propagation from the hot wall adjacent to the thermal chimney throughout the indoor space. As Ri increases, this heat transfer becomes more pronounced, facilitating the movement of heat from hotter to cooler zones. Conversely, when Re rises to 500, the spacing between isotherms increases, indicating the growing influence of forced convection, which enhances both ventilation effectiveness and heat transfer efficiency. The findings also highlight that isotherm density is higher in the upper part of the house, particularly in the dome region, while it decreases in the lower section. This behavior is a result of natural buoyancy, where warmer air rises due to its lower density, while cooler air remains near the floor. Additionally, ventilation from the upper inlet leads to a more uniform temperature distribution across the space, whereas bottom ventilation results in a relatively cooler lower region. The Richardson number (Ri) is a key parameter in evaluating ventilation performance and thermal energy distribution. Its effect on temperature distribution can be categorized as follows: For 2.5 < Ri < 5, forced convection remains dominant, leading to a more uniform temperature distribution. Increased airflow facilitates heat dissipation, preventing localized hot spots. At Ri = 10, buoyancy-driven flow governs the system, causing significant thermal stratification. Warm air accumulates near the ceiling while cooler air remains at the bottom, potentially leading to thermal discomfort and reduced efficiency of heating and cooling processes.

4.3. Local Nusselt number

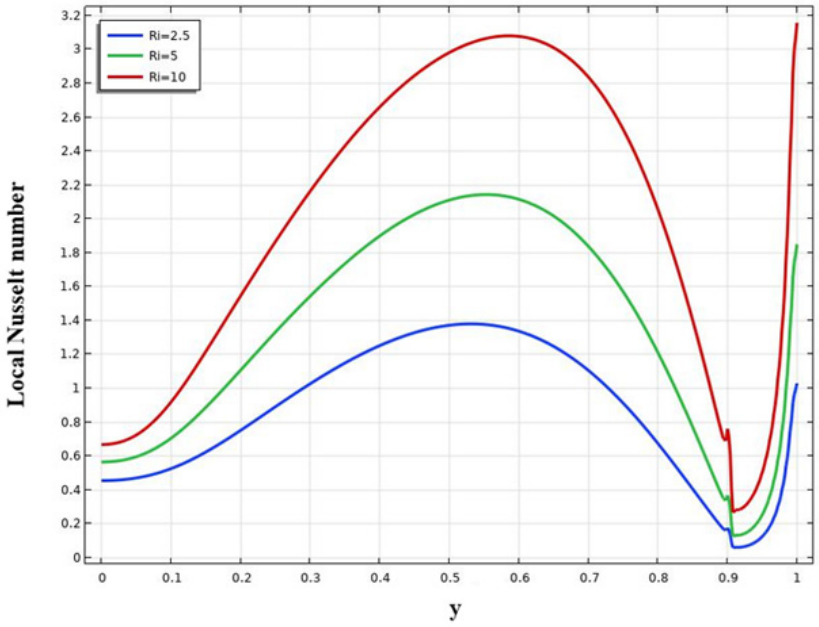

Figure 7. Variation of the local Nusselt number along the cold wall for Case 1. For different Ri and Re=100, Pr=0.71.

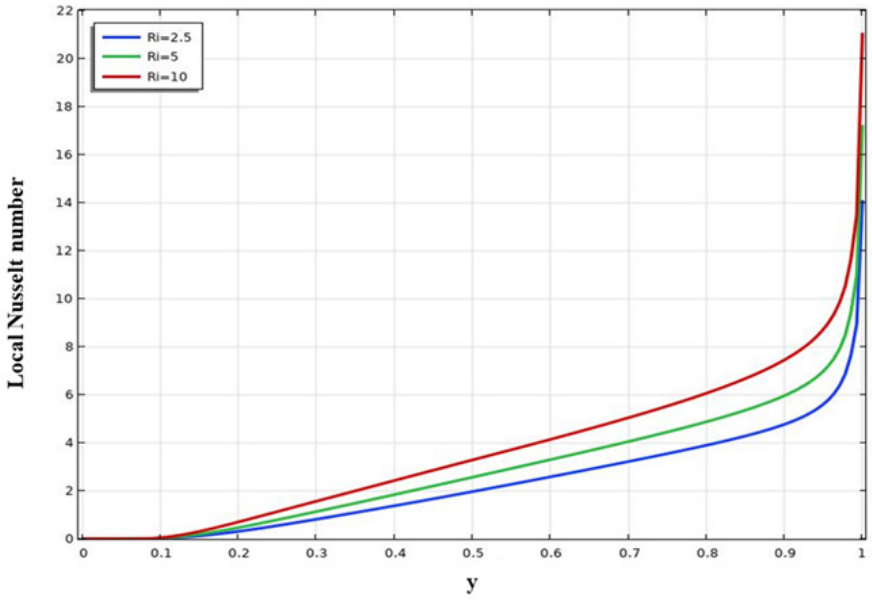

Figure 8. Variation of the local Nusselt number along the cold wall for Case 2. For different Ri and Re=100, Pr=0.71.

Figures 7,8 and 9 show the variation of the local Nusselt number along the cold wall at the ventilation inlet for both the top and bottom ventilation configurations, as well as along the hot wall adjacent to the thermal chimney. These figures highlight the influence of the ventilation inlet position and Richardson number (Ri) on heat transfer characteristics.

For the top ventilation case, the Nusselt number initially shows a low value at the beginning of the cold wall, then increases towards the middle due to heat exchange. After this increase, it gradually decreases before reaching the ventilation inlet at the top, where it rises again due to the effect of the incoming airflow.

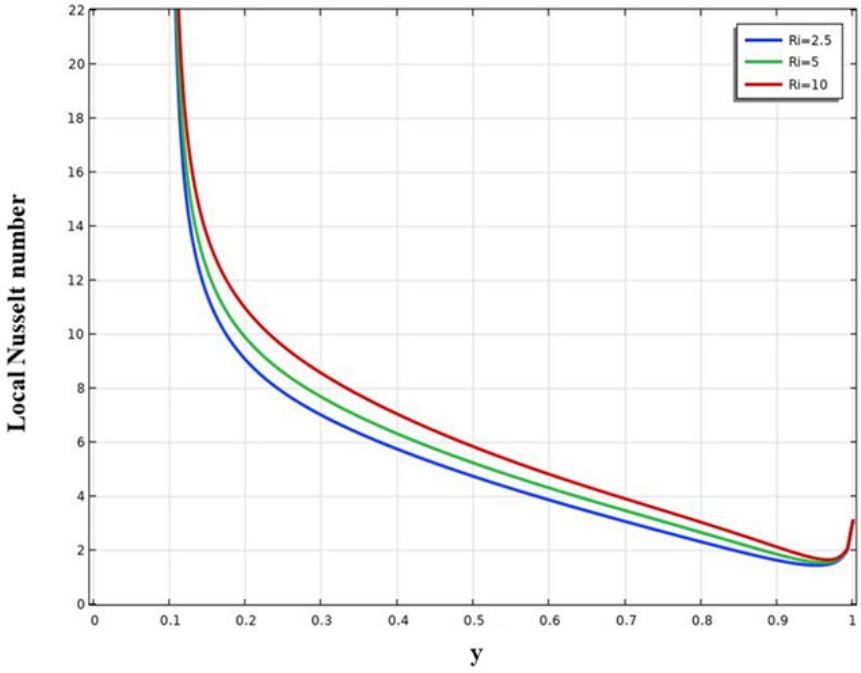

Figure 9. Local Nusselt number on hot walls for different Ri and Re=100, Pr=0.71.

In contrast, for the bottom ventilation configuration, the Nusselt number increases gradually from bottom to top, reaching its maximum value near the top section of the cavity. This trend indicates that heat transfer is significantly affected by the airflow direction and buoyancy effects, resulting in distinct thermal behaviors depending on the ventilation strategy.

For the hot wall, no significant difference is observed when changing the ventilation inlet position. However, the Nusselt number reaches its highest value at the opening connecting the house to the thermal chimney. This increase is attributed to the enhanced heat exchange inside the chimney, which facilitates the removal of hot air and enhances cooling. After this point, the Nusselt number gradually decreases along the upper section of the hot wall. These results confirm the critical role of the chimney in heat dissipation and its impact on the overall thermal performance of the system. Additionally, the results indicate that the Nusselt number (Nu) increases with higher Richardson numbers (Ri), reflecting the influence of buoyancy-driven forces on heat transfer. As Ri increases, natural convection effects become more pronounced, enhancing heat exchange within the cavity. This relationship highlights the strong interplay between buoyancy and forced convection in determining the overall thermal behavior of the system.

4.4. Average Nusselt number

Table 3. Shows the average Nusselt number for different Richardson values at the cold wall. (Re=100 and Pr=0.71).

Ri	2.5	5	10
Nuavg Case 1	2.275	2.891	3.654
Nuavg Case 2	0.860	1.346	1.980

Table 4. Shows the average Nusselt number for different Richardson values at the hot wall.

Ri	2.5	5	10
Nuavg Case 1	4.660	5.235	5.697
Nuavg Case 2	3.971	4.384	4.864

The findings indicate that the average Nusselt number (Nuavg) increases with the Richardson number (Ri) at both the cold and hot walls for the different ventilation configurations, highlighting the significant role of buoyancy-driven convection in enhancing heat transfer. In Case 1, where the ventilation inlet is positioned at the top, Nuavg rises from 2.275 at Ri = 2.5 to 3.654 at Ri = 10 at the cold wall, and from 4.660 to 5.697 at the hot wall, demonstrating that top ventilation facilitates better convective mixing and heat dissipation due to stronger buoyancy effects. Conversely, Case 2, featuring a bottom ventilation inlet, shows considerably lower Nuavg values, increasing from 0.860 to 1.980 at the cold wall and from 3.971 to 4.864 at the hot wall, suggesting that bottom ventilation results in weaker thermal exchange as the incoming cooler air does not interact as effectively with the warmer interior. The higher Nusselt numbers observed in Case 1 confirm that top ventilation enhances natural convection effects more efficiently than bottom ventilation, where heat transfer is less effective. Overall, these results emphasize the critical influence of the ventilation inlet position on heat transfer performance, with buoyancy-driven flow becoming more dominant at higher Ri, particularly when ventilation is sourced from the top, thereby enhancing heat dissipation in the system.

5. CONCLUSION

This study emphasizes the significant role of solar energy in improving natural ventilation in buildings through the use of a solar chimney. The solar chimney is essential for enhancing cooling efficiency by boosting natural airflow within structures. The findings show that the placement of the ventilation inlet greatly impacts airflow dynamics and heat transfer. Notably, top ventilation enhances airflow, increases heat removal, and improves overall ventilation efficiency compared to bottom ventilation.

At lower Richardson numbers ($2.5 \leq Ri < 5$), forced convection is predominant, resulting in higher airflow velocities and more uniform temperature distribution. As Ri rises to 10, buoyancy-driven convection becomes more significant, leading to stronger thermal stratification within the space. Furthermore, increasing the Reynolds number from 100 to 500 boosts convective heat transfer, particularly in Case 1, where intensified airflow promotes better mixing and more effective heat dissipation. The solar chimney plays a crucial role by generating buoyancy effects, aiding the upward movement of warm air and expelling it from the interior, thereby enhancing the ventilation system's overall performance.

The solar chimney illustrates a practical application of solar energy in architectural design. Optimizing its orientation, height, and solar exposure area can substantially improve its thermal performance. This allows the chimney to capture solar energy effectively, stimulate natural airflow, minimize dependence on mechanical ventilation, and enhance the building's energy efficiency. Consequently, the solar chimney acts as an efficient passive cooling system and sustainable energy solution, supporting the advancement of energy-efficient residential architecture.

Author Contributions: All authors have made a substantial, direct, and intellectual contribution to the work and approved it for publication.
Funding: There is no funding for the article.
Data Availability Statement: The data are available at request.
Conflicts of Interest: The authors declare no conflicts of interest.

REFERENCES

[1] A. A. Aqila, Y. F. Nassar, H. El-Khozondar, and S. Suliman, "Design of Hybrid Renewable Energy System (PV/Wind/Battery) Under Real Climatic and Operational Conditions to Meet Full

Load of the Residential Sector: A Case Study of a House in Samno Village– Southern Region of Libya," Wadi Alshatti University Journal of Pure and Applied Sciences, pp. 168–168, Apr. 2025.

[2] "Algeria - Countries & Regions," IEA. https://www.iea.org/countries/algeria/electricity.

[3] P. Lotfabadi, "Analyzing passive solar strategies in the case of high-rise building," Renewable and Sustainable Energy Reviews, vol. 52, pp. 1340–1353, Dec. 2015.

[4] Z. Dicka, E. Dolnikova, and D. Katunsky, "Solar architecture: Significance and integration of technologies," E3S Web of Conferences, vol. 550, p. 01002, 2024

[5] C. Vassiliades, S. Kalogirou, A. Michael, and A. Savvides, "A Roadmap for the Integration of Active Solar Systems into Buildings," Applied Sciences, vol. 9, no. 12, p. 2462, Jun. 2019.

[6] D. Stankovic, "Improvement of Energy Efficiency of Schools and Kindergartens," MATEC Web of Conferences, vol. 53, p. 01018, 2016.

[7] G. Ren, X. Zhao, C. Zhan, H. Jin, and A. Zhou, "Investigation of the Energy Performance of a Novel Modular Solar Building Envelope," Energies, vol. 10, no. 7, p. 880, Jun. 2017.

[8] N. Aboud, "Integration of Photovoltaic Cells in Building Shading Devices":, Solar Energy and Sustainable Development Journal, vol. 13, no. 2, pp. 83–101, Jul. 2024.

[9] G. Ren, X. Zhao, C. Zhan, H. Jin, and A. Zhou, "Investigation of the Energy Performance of a Novel Modular Solar Building Envelope," Energies, vol. 10, no. 7, p. 880, Jun. 2017.

[10] Y. Q. Nguyen, T. N. Huynh, and M.-A. H. Pham, "Modifications of Heat Transfer and Induced Flow Rate of a Solar Chimney by an Obstacle in the Air Channel," International Journal on Advanced Science Engineering and Information Technology, vol. 11, no. 2, pp. 482–488, Apr. 2021.

[11] R. A. Ibrahim, P. Tittelein, S. Lassue, F. H. Chehade, and L. Zalewski, "New Supply-Air Solar Wall with Thermal Storage Designed to Preheat Fresh Air: Development of a Numerical Model Adapted to Building Energy Simulation," Applied Sciences, vol. 12, no. 8, p. 3986, Apr. 2022.

[12] S. Ihfedah, M. Al-Madani, and S. Gnefid, "Techno-Economic Analysis of Solar Energy Developing Technologies in Libyan Residential Communities," Solar Energy and Sustainable Development Journal, vol. 14, no. FICTS-2024, pp. 137–164, Jan. 2025.

[13] J. Chen, G. S. Brager, G. Augenbroe, and X. Song, "Impact of outdoor air quality on the natural ventilation usage of commercial buildings in the US," Applied Energy, vol. 235, pp. 673–684, Feb. 2019.

[14] Y. Chen, Z. Tong, W. Wu, H. Samuelson, A. Malkawi, and L. Norford, "Achieving natural ventilation potential in practice: Control schemes and levels of automation," Applied Energy, vol. 235, pp. 1141–1152, Feb. 2019.

[15] S. Brito-Coimbra, D. Aelenei, M. Gloria Gomes, and A. Moret Rodrigues, "Building Façade Retrofit with Solar Passive Technologies: A Literature Review," Energies, vol. 14, no. 6, p. 1774, Mar. 2021.

[16] C. E. Brahmi, M. M. Battira, N. Belghar, M. Kalfali, and R. Bessaih, "Free convection and entropy generation inside porous cavities with irregular vertical walls nonuniformly heated from below," Numerical heat transfer. Part A. Applications/Numerical heat transfer. Part A, Applications, pp. 1–27, May 2024.

[17] C. E. Brahmi, M. M. Battira, N. Belghar, and M. Kalfali, "Natural convection within a greenhouse cavity with a porous layer mimicking Algerian soil heated by embedded hot pipes: effects of soil porosity and permeability," STUDIES IN ENGINEERING AND EXACT SCIENCES, vol. 5, no. 2, pp. e11657–e11657, Dec. 2024.

[18] R. Bassiouny and N. S. A. Koura, "An analytical and numerical study of solar chimney use for room natural ventilation," Energy and Buildings, vol. 40, no. 5, pp. 865–873, Jan. 2008.

[19] M. Kalfali, M. M. Battira, N. Belghar, and C. E. Brahmi, "Optimizing thermal management in buildings: the role of mixed convection and solar chimneys," STUDIES IN ENGINEERING AND EXACT SCIENCES, vol. 5, no. 3, pp. e12886–e12886, Dec. 2024 Please find attached the revised manuscript along with the signed copyright transfer form for your consideration.

[20] L. Shi, G. Zhang, W. Yang, D. Huang, X. Cheng, and S. Setunge, "Determining the influencing factors on the performance of solar chimney in buildings," Renewable and Sustainable Energy Reviews, vol. 88, pp. 223–238, May 2018.

[21] A. J. Chamkha, Salam Hadi Hussain, and Qusay Rashid Abd-Amer, "Mixed Convection Heat Transfer of Air inside a Square Vented Cavity with a Heated Horizontal Square Cylinder," Numerical Heat Transfer Part A-applications, vol. 59, no. 1, pp. 58–79, Jan. 2011.

[22] Saha, S., Mamun, A. H., Hossein, M. Z., & SADR, A. A. (2008). Mixed convection in an enclosure with different inlet and exit configurations.

[23] M. M. Rahman, M. A. Alim, S. Saha, and M. K. Chowdhury, "A numerical study of mixed convection in a square cavity with a heat conducting square cylinder at different locations," Journal of Mechanical Engineering, vol. 39, no. 2, pp. 78–85, 2008.

[24] S. Bhardwaj, A. Dalal, and S. Pati, "Influence of wavy wall and non-uniform heating on natural convection heat transfer and entropy generation inside porous complex enclosure," Energy, vol. 79, pp. 467–481, Jan. 2015.

[25] S. Kundu, S. Haydar, and P. Mandal, "Zinc Oxide Nanoparticles: Different synthesis approaches and applications," NBU journal of plant sciences, vol. 13, no. 1, pp. 42–64, Jan. 2021.

[26] C. E. Brahmi, M. M. Battira, N. Belghar, M. Kalfali, and Z. Driss, "Free Convection inside Greenhouse Cavity Partially Filled with Bottom Porous Layer: The Influence of Soil's Porosity and Permeability," International Journal of Heat and Technology, vol. 42, no. 6, pp. 1849–1858, Dec. 2024.

NOMENCLATURE

Pr: Prandtl number	β: thermal expansion coefficient, 1/K.
Re: Reynolds number	L: Length of the cavity.
Ri: Richardson number	g: gravitational acceleration, m/s^2.
Nu: Nusselt number	X, Y: dimensionless Cartesian coordinates
K: thermal conductivity of fluid, W/m°C.	U: dimensionless velocity component in x-direction.
α: thermal diffusivity, m^2/s.	V: dimensionless velocity component in y-direction.
υ: kinematic viscosity, m^2/s	θ: dimensionless temperature.
T: dimensional temperature, C	
P : dimensional pressure, N/m^2	
ρ: density of the fluid, kg/m^3.	